Sauvain, J.J.; Rossi, M.J. **Quantitative aspects of the interfacial catalytic oxidation of dithiothreitol by dissolved oxygen in the presence of carbon nanoparticles**. Environmental Science & Technology 50(2):996-1004, 2016.

Postprint version	Final draft post-refereeing
Journal website	http://pubs.acs.org/journal/esthag
Pubmed link	http://www.ncbi.nlm.nih.gov/pubmed/26683500
DOI	10.1021/acs.est.5b04958

Quantitative aspects of the interfacial catalytic oxidation of Dithiothreitol by dissolved oxygen in the presence of carbon nanoparticles.

Jean-Jacques Sauvain[1]*, *Michel J. Rossi*[2]

[1] Institute for Work and Health (IST), University of Lausanne and Geneva, Route de la Corniche 2, CH-1066 Epalinges-Lausanne, Switzerland

[2] Paul Scherrer Institute (PSI), Laboratory of Atmospheric Chemistry (LAC), CH-5232 Villigen PSI, Switzerland

* : Corresponding author.

E-mail address : jean-jacques.sauvain@hospvd.ch Tel : +41 21 314 74 34

ABSTRACT

The catalytic nature of particulate matter is often advocated to explain its ability to generate reactive oxygen species, but quantitative data are lacking. We have performed molecular characterization of three different carbonaceous nanoparticles (NP) by: 1. identifying and quantifying their surface functional groups based on probe gas-particle titration; 2. studying the kinetics of dissolved oxygen consumption in the presence of suspended NP's and dithiothreitol (DTT). We show that these NP's can reversibly change their oxidation state between oxidized and reduced functional groups present on the NP surface. By comparing the amount of O_2 consumed and the number of strongly reducing sites on the NP, its average turnover ranged from 35 to 600 depending on the type of NP. The observed quadratic rate law for O_2 disappearance points to a Langmuir-Hinshelwood surface-based reaction mechanism possibly involving semiquinone radical. In the proposed model, the strongly reducing surface site is assumed to be a polycyclic aromatic conjugated hydroquinone whose oxidation to the corresponding quinone is rate-limiting in the catalytic chain reaction. The presence and strength of the reducing surface functional groups are important for explaining the catalytic activity of NP in the presence of oxygen and a reducing agent like DTT.

TOC / ABSTRACT GRAPHIC

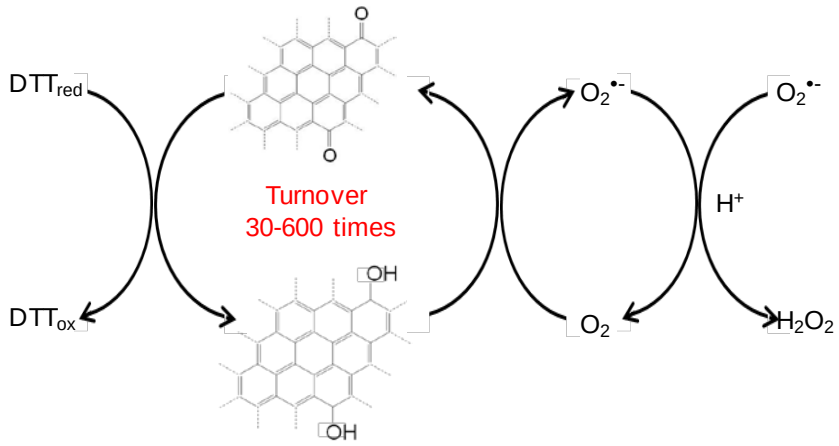

INTRODUCTION

Oxidative stress is now recognized as a very important mechanism that possibly explains the effect of particulate matter (PM) on health.[1] Oxidative stress can be defined as the uncontrolled production of reactive oxygen species (ROS, like $OH^{\bullet}$, $O_2^{\bullet-}$, $HO_2^{\bullet}$, $HO_2^{\bullet-}$, H_2O_2, etc.) at the cellular level, modifying the biological redox balance, and inducing a sequential upregulation of the synthesis of defense enzymes (antioxidants) followed by inflammation processes when defenses are overwhelmed which eventually lead to cellular toxicity.[2]

One often advocated hypothesis that explains how a small amount of deposited particles in the reducing environment of the lungs[3] can generate a large amount of ROS is that particles act through interfacial (heterogeneous) catalysis and are able to maintain a ROS production in biological systems.[4-6] Such processes have often been reported for acellular assays involving ambient particles and occurring in a reducing environment containing molecular oxygen.[7-9] By definition, a heterogeneous catalyst consists of a solid which will modify the reaction kinetics between two reactants, without being consumed itself and thus changing the global stoichiometry. Two main features are noteworthy: 1. The catalyst controls certain elementary

steps, usually by increasing its specific rate constants, for instance for oxidation; 2. The catalyst is continuously restored to its original state after reaction in what is called redox-cycling when the catalyst returns to its initial oxidation state; such a reaction-regeneration or redox cycle occurs many times with the catalyst and corresponds to its turnover. From a molecular point of view, turnover is defined in the present case as the ratio of O_2 consumed to the number of reducing catalytic sites involved at the nanoparticle interface. The way and where these ROS are formed is still not clearly understood, but particulate surface redox cycling of metal ions,[10,11] quinones,[12-15] or "environmentally persistent free radicals" (EPFR)[4, 16, 17] are often advocated for ambient particles. In addition, such a redox activity has been shown to partition between the (water/organic) soluble fraction and the insoluble elemental carbon core[8,9] for ambient particles. Such a phase partitioning may be quite variable, depending on the PM composition, photochemical processes (oxidation and aging) and particle surface properties.[9] The chemical mechanism[6, 18] includes reactions of redox active compounds and/or surface functionalities on the particle surface that reduce molecular oxygen to superoxide anion ($O_2^{\bullet -}$) in a single electron transfer step coupled to subsequent regeneration of the redox active species/function by reducing agents present in the environment. Whereas such a catalytic redox activity of PM is mentioned to take place "many times",[6] very few studies report on a quantitative evaluation of the turnover number or frequency for such a process. Khachatryan et al.[19] reported that 1 EPFR generated approximately 10 $OH^{\bullet}$ free radicals for the model system 2-monochlorophenol associated with copper oxide-containing silica particles in phosphate buffered saline. A number of investigators prefer not to identify the specific redox reactions at hand and generally refer to redox cycling of reactive sites located at particle interfaces without giving proof of evidence.[5-8] There is a clear need for understanding how such a catalytic activity arises[9] including the identification of the

chain carriers active in the redox-cycling oxidative chain reaction. The investigation of the reactivity of the particle (catalyst) redox-active sites involved in the change of oxidation state during reaction is thus necessary.

Dithiothreitol (DTT) is a strong reducing agent and is very often used to probe the oxidizing behavior of bioorganic systems in solution as well as in an assay format for reactivity testing of particles.[1] The mechanism of DTT oxidation is complex and radical-induced oxidation chemistry has been demonstrated under radiolytic conditions[20, 21] or in the presence of metal ions,[22, 23] involving oxygen and sulfur-based free radical intermediates. Previous work in our laboratory indicated that such catalytic processes may take place in the DTT assay in the presence of different carbon black (CB) and diesel particulates.[24] The most important observation was that the presence of strongly reducing surface functional groups (probed with the weak oxidizer NO_2) apparently are associated with the DTT consumption rate.

In this paper, we present quantitative data regarding the kinetic characteristics of the catalytic surface process between carbonaceous nanoparticles and DTT in the presence of dissolved oxygen in aqueous solution. More specifically, we display the rate law for the radical chain reaction for oxidation of DTT in the presence of an aqueous suspension of carbonaceous (soot and amorphous carbon) nanoparticles (NP), chain reaction overall stoichiometry and chain length for different NP substrates. We propose an overall mechanism for this particular system and a quantitative framework for the understanding of the catalytic chain oxidation of a model antioxidant by particles is presented.

EXPERIMENTAL SECTION

Nanoparticles and chemicals

Two different CB NPs (FW2 and Printex 90, both from Evonik, Germany) and one reference diesel material (SRM 2975, Promochem, Germany) were used in this study. These particles presented different surface polarities (FW2 being more oxidized than Printex 90, with SRM 2975 being intermediate) and may be considered as particles mainly composed of elemental carbon with a low mass of adsorbed organics (less than 6% by weight).[24] The extractable organic fraction in dichloromethane is reported to be 2.7±0.2%[25] for SRM 2975. Particle characteristics have already been published.[24] The Supporting Information Section, Table S1 lists the experimental decay rates of DTT and O_2 in aqueous solution as well as the type and quantity of relevant surface functional groups of the three investigated carbonaceous NP materials.

The particles were suspended in water containing the non-ionic surfactant polyoxyethylene sorbitanmonooleate (Tween 80®, Fluka) at a concentration of 0.6 mg L^{-1}. Just prior to conducting the DTT assay, a stock suspension of 50 mg L^{-1} of NP was prepared in 0.6 mg L^{-1} Tween 80® and sonicated for 15 minutes at 180 W in a water bath set at 30°C. Further dilution of the stock particle suspension with the same media followed by a 15 minute sonication was performed in order to obtain final particle concentrations between 4-50 mg L^{-1}.[26]

In anticipation of the results of the present study and as reported by others,[27, 28] the oxidation-reduction reactions take place on the particle surface. Therefore, the chemical reactivity at the interface of carbonaceous NP's were characterized in terms of surface functional groups using chemical titration at molecular flow conditions in a Knudsen reactor, as described by Setyan et al.[29] Briefly, a molecular flow of a reactive probing gas is passed through a reactor containing the sample to specifically interact with functional groups on the surface of the particle during its gas-residence time. The temporary decrease of the exiting gas flow is recorded and can be related to the number of reacting sites on the particle. We used four different gas probes (trimethylamine

$N(CH_3)_3$, hydroxylamine NH_2OH, ozone O_3 and nitrogen dioxide NO_2) to titrate Brönsted/Lewis acids, carbonyls/electrophiles, sum of reducing and strongly reducing surface functional groups, respectively (see Supporting Information, Table S1). The strongly reducing surface functional groups correspond thus to a subgroup in the sum of all reducing functional groups on the NP surface. Additional characterization of the particulate surface has been performed by Fourier transform infra-red (FTIR) spectroscopy. The FTIR spectra of the soot samples were recorded in the range 4000 - 500 cm^{-1} on a Varian FTIR-Excalibur spectrometer using the KBr pellet technique. The particle concentration in the KBr pellet was comprised between 0.03-0.16% (wt). Before measurement, the ground mixture was heated overnight in an oven set at 105°C, in order to evaporate adsorbed water. A total of 10 scans were co-added at a spectral resolution of 4 cm^{-1}.

O_2 and DTT consumption assay

The kinetics of oxygen consumption in the reacting system DTT - NP- O_2 has been studied in an air-tight reactor (total volume 14.3 ml) using a Clark electrode as sensor (Oxi 340i, WTW, Germany). The sensor was calibrated on a daily basis, by putting it in an air-saturated aqueous environment at ambient temperature. The reactor consisted of a screw cap tube with two side arms capped with silicone septa (see Supporting Information, Figure S1). After filling the reactor with a phosphate buffer (62 mM, pH 7.4), containing 7 mg L^{-1} Tween 80®, the calibrated Clark electrode was passed through an O-ring-sealed screw cap and the system was tightly closed by taking care to avoid air bubbles. A needle connected to a Teflon lid was introduced through the septum of one sidearm in order to discard excess solution during the injection of reactants which took place from the other sidearm. Once the magnetic stirrer was switched on, the oxygen concentration was recorded until stabilization (approximately 8 mg L^{-1}, 10 minutes). A typical experiment was performed in two steps: First, the initial oxygen consumption rate in the

presence of DTT only (R_{ox}DTT) was measured. The Teflon lid was briefly opened, 50 µl of 28 mM DTT standard solution (corresponding to 100 µM in the reactor) was injected through one side arm using a syringe and the lid closed thereafter. The slow decrease of O_2 concentration was recorded every minute during at least 15 minutes; Second, the oxygen consumption was measured in the presence of particles. Without interrupting the monitoring of the oxygen concentration, the Teflon lid was opened again, 1 ml of the particle suspension was injected from the opposite arm and the lid eventually closed. The decrease of the O_2 concentration in the reactor was recorded until a constant O_2 concentration was observed. In order to demonstrate that PM was still reactive in this system, we successively added aliquots of 50 µl of the standard DTT solution, once or twice for Printex 90 and FW2, respectively, and the decrease of O_2 concentration was again recorded. The experimental design allowed us to determine the initial O_2 consumption rate at different dissolved oxygen concentrations. We also verified that the injection of particle suspensions without DTT did not lead to a change in the dissolved O_2 concentration as a function of time (data not shown).

The DTT consumption was determined following a published method.[26] Briefly, 5 ml of DTT 100 µM in 0.1M phosphate buffer pH 7.4 and 5 ml of particles suspension were incubated at 37°C with magnetic stirring. At different times (approximately every 5-10 min during 60 min), 500 µl of the reacting solution was taken and the non-oxidized DTT content determined by reaction with 10 mM of 5,5'-dithiobis(2-nitrobenzoic acid) in water. The resulting 5-mercapto-2-nitrobenzoic acid was determined colorimetrically at 412 nm. Blank runs in absence of suspended NP's were performed in parallel in order to correct for the rate of DTT consumption in the slow auto-oxidation of DTT.

Data treatment

The initial rate of dissolved oxygen consumption (R_{ox}) was calculated from the slope of the initial [O_2] traces. It was corrected for R_{ox}DTT determined in the absence of solid particles by simple subtraction of the (measured) background from the measured sample rate. The initial rate of O_2 consumption measured as the tangent of the recorded and calibrated O_2 concentration at t = 0 therefore corresponds to the initial sample rate in the presence of suspended carbonaceous particles.

RESULTS AND DISCUSSION

Experimental rate of O_2 consumption

Figure 1 shows a typical example of the dissolved O_2 concentration as a function of a triple sequential addition of DTT in the presence of a FW2 suspension. At t = 21 minutes an aliquot of DTT is added in the absence of FW2 without visible effect on [O_2]. After injection of 1 ml of aqueous FW2 suspension, O_2 starts to decrease until all DTT has been consumed. At t = 68 minutes a second identical amount of DTT was added at a lower measured O_2 concentration accompanied by a significant decrease of [O_2]. Finally at t = 104 minutes a third identical amount of DTT was added which led to another decrease of [O_2]. Obviously, we did not wait long enough after the third addition of DTT in order to reveal the asymptotic level of [O_2] because the experiment was terminated at t = 135 minutes. The simultaneous presence of DTT and an aqueous suspension of FW2 is required in order to observe a measurable decrease of [O_2]. The initial slope of [O_2] as a function of time (Table 1) corresponds to the rate of initial O_2 consumption, which decreases after each addition of DTT owing to the decreasing level of [O_2] in solution.

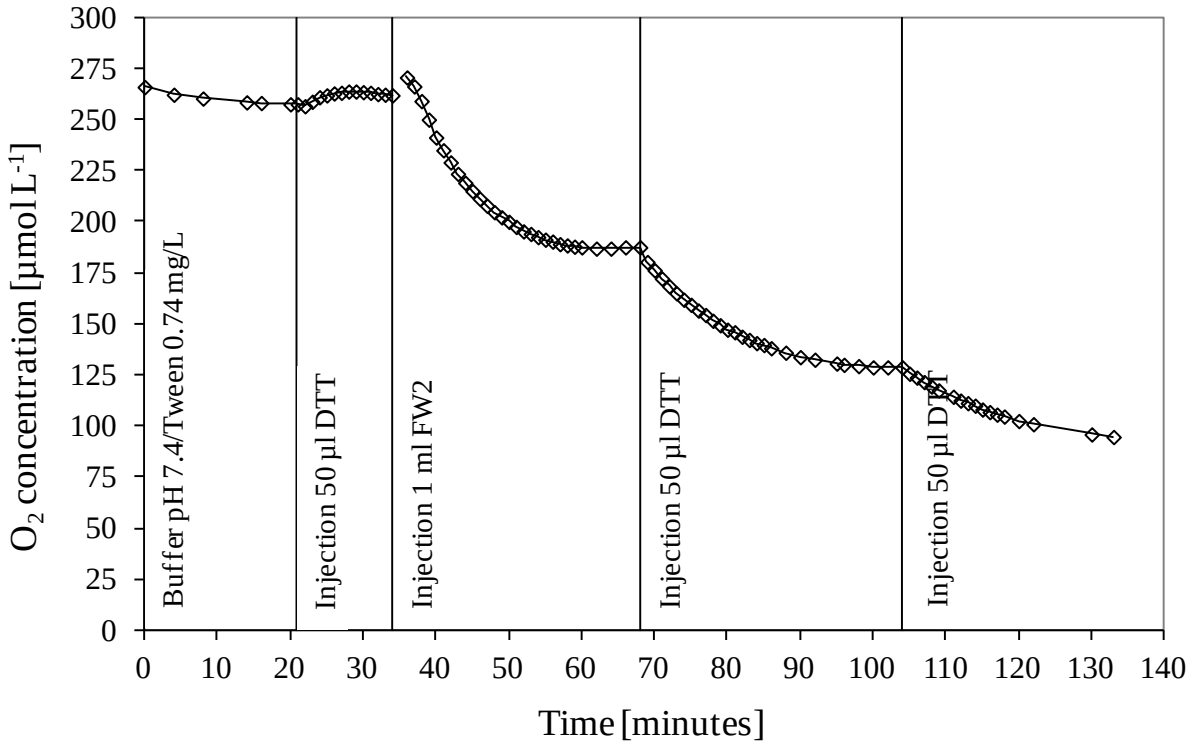

Figure 1: Typical response of the calibrated Clark oxygen electrode to a single addition of amorphous carbon suspension (initial concentrations in the reactor: FW2 27 mg/L) and three sequential, albeit identical amounts of DTT (initial concentration of DTT in the reactor: 113 µM). Conditions: pH: 7.4; Tween 80®: 0.74 mg L^{-1}, T: 25°C. The initial O_2 level corresponds to saturation in water at 298 K corresponding to a Henry's law constant of H_{cp} = 1.3x10^{-5} mol m^{-3} Pa or 1.32 x 10^{-3} M atm^{-1} or 264 µM in 1 atmosphere of air (20% (v/v) O_2).[30]

The averaged value for the initial oxidation of 100 µM DTT alone (R_{ox}DTT) observed for all the tests was as low as 0.33±0.18 µM min^{-1} (n=19). All consumption rates of DTT in the presence of NP's (R_{ox}) were corrected using this value. Table 1 presents the averaged initial rates of O_2 consumption for the three types of investigated particles when DTT is injected in a repetitive way (total of three injections for FW2, two for Printex 90 and one for SRM 2975).

Table 1: Initial rate of O_2 consumption (with standard deviation) for the three amorphous carbons studied. Two and one identical subsequent additions of DTT have been performed for FW2 and Printex 90, respectively. The third column displays the acceleration of the O_2 consumption rate in the presence of particles (R_{ox}) compared to the corresponding control run without particles (R_{ox}DTT). Conditions in the reacting media: DTT: 100 µM; particle: 27 mg L^{-1}; phosphate buffer 62 mM, pH 7.4.

	n	Initial rate O_2 consumption (R_{ox}) [µmol O_2 L^{-1} min^{-1}]	Initial rate (mass normalised) O_2 consumption (R_{ox}/M) [µmol O_2 L^{-1} min^{-1} mg^{-1}]	Ratio R_{ox}/R_{ox}DTT
R_{ox}DTT (no particles)	19	0.3 ± 0.2	-	-
FW2 (1st inj)	9	6.1 ± 2.5	17.4 ± 4.5	18.7
FW2 (2nd inj)	5	3.0 ± 1.4	8.6 ± 3.1	9.2
FW2 (3nd inj)	3	2.1 ± 0.6	5.8 ± 1.5	6.5
Printex 90 (1st inj)	4	2.8 ± 2.4	6.4 ± 4.4	8.6
Printex 90 (2nd inj)	2	1.0 ± 0.4	2.4 ± 1.6	2.9
SRM 2975	4	1.8 ± 0.7	3.8 ± 1.9	5.4

As shown in Table 1 for first injections of DTT and depending on [O_2], the decay rate of dissolved O_2 is approximately 6-20 times faster in the presence of NP compared to without at an average particle loading of 27 mg L^{-1}.

DTT decay in the presence of an aqueous suspension of carbon nanoparticles

The plot of [DTT] = f(t) has always been observed to be linear or quasi-linear in the time range considered (0-60 min) under all experimental conditions, at variance with the expected exponential decay.[26] The DTT disappearance rate at an initial DTT concentration of 50 µM is also a function of the particle mass (from 0-8 mg L^{-1}) that linearly correlates with the DTT rate of disappearance (Figure 2).

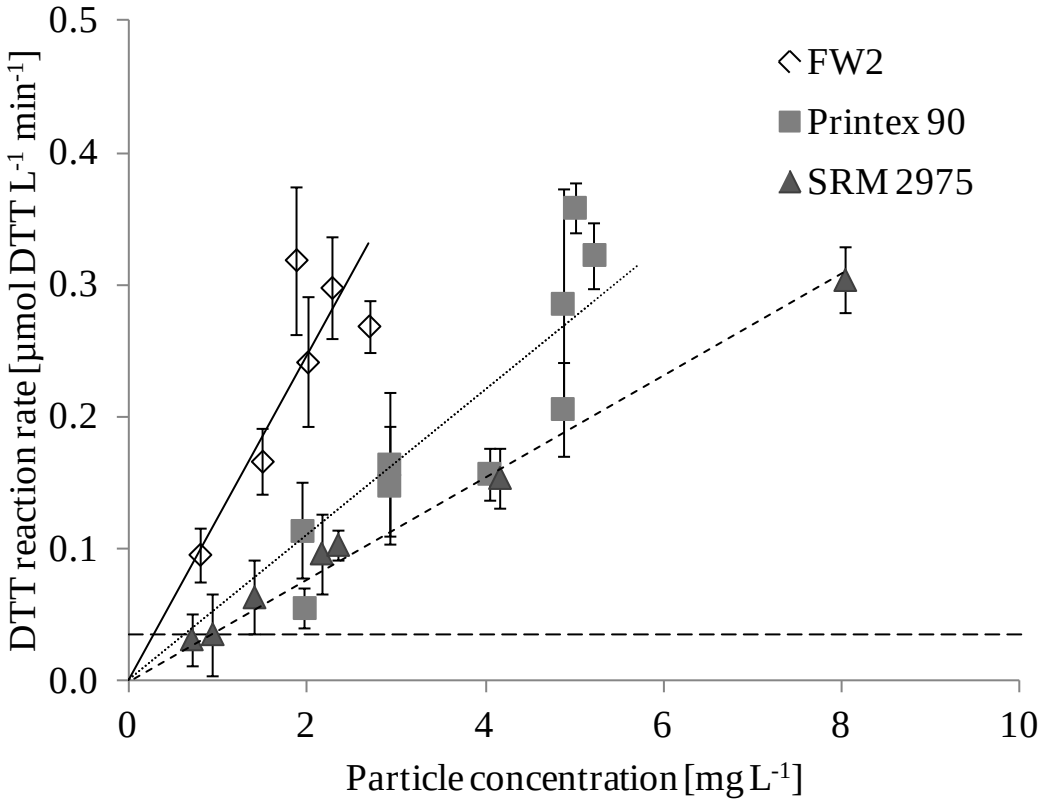

Figure 2: Plot of the DTT consumption rate in aqueous solution at ambient temperature as a function of the mass-based concentration of the displayed particles. The least-squares straight line through the origin corresponds to the mass-based DTT reactivity (µmol DTT min^{-1} mg^{-1}). The horizontal dotted line corresponds to the estimated limit of detection, corresponding to 3 times the standard deviation of the blank.

The slope of this correlation or the initial ratio of the DTT consumption rate to the NP mass is thus a constant and may be considered a particle characteristic. If the NP mass concentration in Figure 2 is replaced with the NP surface concentration we also obtain a significant linear dependence (not shown), however the resulting sequence of the rate coefficient, namely SRM 2975 > FW2 > Printex 90 is reversed from the order FW2 > Printex 90 > SRM 2975 displayed in

Figure 2. The obvious reason is attributed to the different value of the absolute surface-to-volume ratio as measured by the Brunauer-Emmett-Teller (BET) specific surface area (Table S1, Supporting Information). In addition, the initial DTT consumption rate is proportional to the initial DTT concentration under the present conditions (see Supporting Information, Figure S2). The linear decay kinetics of DTT in contrast to the O_2 decay is presently not understood, nevertheless it has been observed by several workers.[5, 7, 9, 23] However, the DTT decay kinetics was not the focus of the present study, rather we emphasize here the O_2 decay kinetics in the presence of DTT and suspended NP's. The oxidation of DTT is reasonably fast both under acidic and basic conditions,[20-23] however, it is a complex chain reaction with many different pathways and numerous intermediates that will be studied in greater detail at a later stage.

Stoichiometry of the reaction in relation to DTT and O_2

Based on the established reaction of DTT oxidation by oxygen,[7, 20] we expect a stoichiometry of 2 : 1 (DTT : O_2), as indicated by reaction (A) being the sum of the partial reactions (1) – (3):

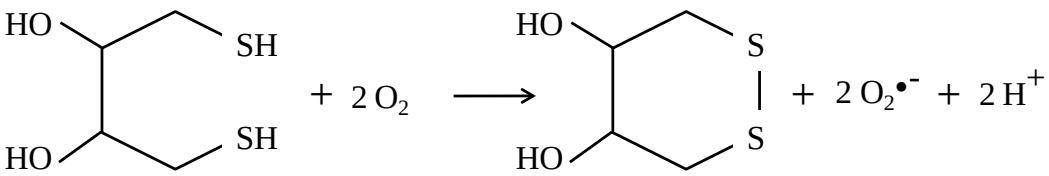

(1)

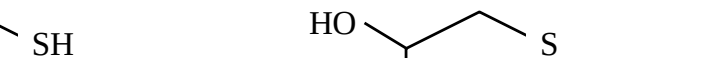

(2)

(3)

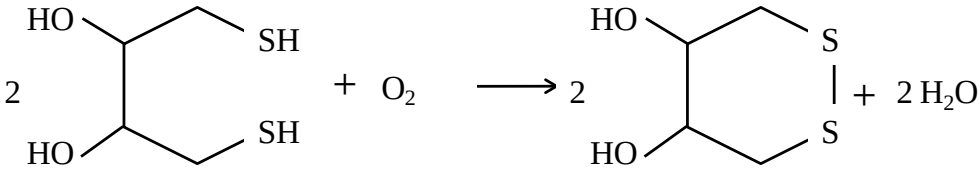

(A)

Assuming that all the added DTT reacted quantitatively as suggested in Figure 1 where the O_2 consumption ceased after a given amount of time after each addition of DTT, the stoichiometric ratio was calculated based on the amount of DTT added and therefore available for reaction as a function of the amount of oxygen consumed ($[DTT]_0/\Delta[O_2]$, Figure 3). An experimental stoichiometric ratio $[DTT]_0/\Delta[O_2]$ = 1.5 ± 0.3, 1.2 ± 0.2 and 1.6 ± 0.2 is determined for FW2, Printex 90 and SRM 2975, respectively. In addition, Figure 3 shows that the measured stoichiometry is similar for all three types of NP within the uncertainty of the experimental technique. The overall oxidation of DTT by oxygen (reaction A) is thermodynamically favorable as E_0 (DTT_{ox}/DTT) = - 0.33 V and E_0 (O_2/H_2O) = + 1.229 V[31] but kinetically slow because of slow steps in the molecular mechanism.[32]

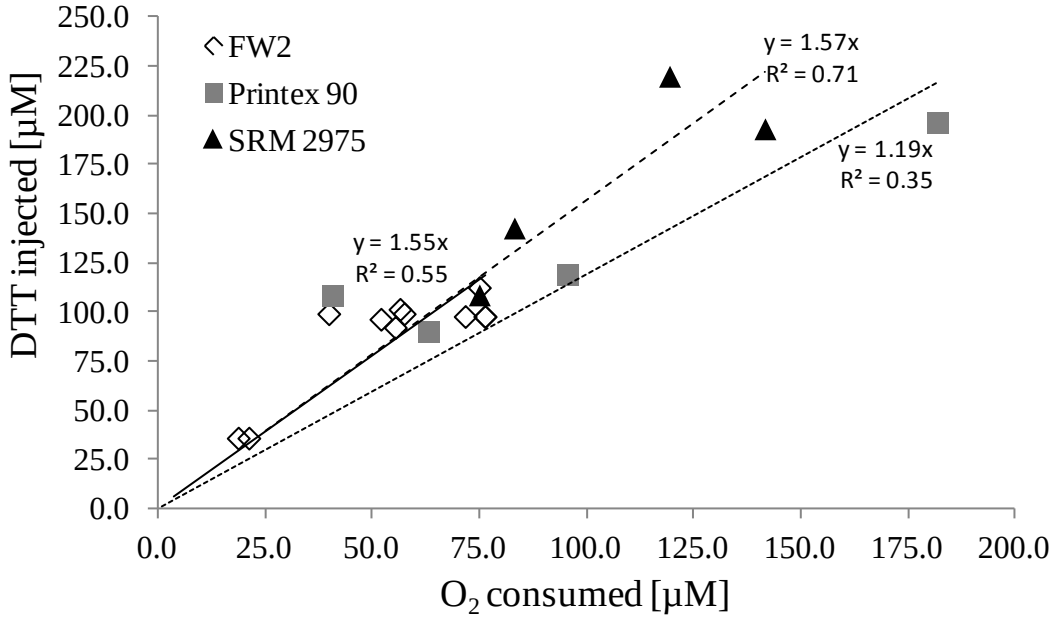

Figure 3: Number of DTT molecules present in solution and plotted against O_2 molecules consumed. Least squares lines are forced through the origin.

The fact that the experimental ratio of total DTT available to O_2 consumed for each particle is smaller than the ideal value of 2.0 according to the simple scheme (A) suggests that on average we have a shortfall of 25 - 40% of DTT that is not oxidized. In other terms, the consumed O_2 is reacting with another reactant instead of DTT. O_2, but more probably one of its reaction intermediates, is apparently reacting with another species instead of DTT. During the redox process, $O_2^{\bullet-}$ and H_2O_2 are generated, which can further react with other components present in solution. Reaction between DTT and H_2O_2 has been reported by different authors.[11, 12, 26, 33] In order to accommodate the loss of DTT oxidation relative to O_2 consumed, we propose the following additional reaction which takes into account the experimentally measured stoichiometry of less than two molecules of DTT per O_2 consumed:

$$d\ H_2O_2 + d\ DTT \rightarrow d\ DTT_{ox} + 2\ d\ H_2O \qquad (4)$$

$$(1 - d)\ H_2O_2 + (1 - d)\ PM \rightarrow (1 - d)\ PM_{oxx} + 2\ (1- d)\ H_2O \quad (5)$$

where PM_{oxx} may be identified with an irreversibly oxidized NP site that is lost for reversible redox cycling and therefore represents a loss of catalyst. Given the nature of the carbonaceous substrate there should be many available oxidizable sites where H_2O_2 may be consumed. Table S1 in the Supporting Information reveals that the strongly reducing surface groups represent 1.3, 1.6 and 0.5% of a formal monolayer of adsorbed NO_2 for FW2, Printex 90 and SRM 2975, respectively. However, the sum of all oxidizable sites is significantly larger than the strongly reducing sites by factors of 3 to 20 (Supporting Information, Table S1) so that H_2O_2 may be reduced by many reducing sites other than the available strongly reducing sites. Every H_2O_2 consumed in reaction (5) will decrease the oxidation yield of DTT because it will not be available to oxidize DTT in reaction (4). Instead, H_2O_2 is consumed on one of the many existing reduced sites of the carbon nanoparticle that will therefore not participate in redox cycling anymore and thereby represents a loss of oxidizer. Parameter d is a number between 0 and 1 where $d = 1.0$ corresponds to the simple mechanism (3) whereas $d = 0$ corresponds to a situation where all H_2O_2 is consumed in order to generate PM_{oxx} resulting in $[DTT]/\Delta[O_2] = 1.0$. The branching ratio $d/(1 - d)$ therefore controls the numerical value of $[DTT]_0/\Delta\ [O_2]$.

Catalytic activity

The observed increase of O_2 consumption in presence of DTT and particles compared to without particles (Table 1) imply that reducing functional groups present on the particle surface are involved in the DTT oxidation process by dissolved O_2. In a previous paper from our laboratory,[24] different surface functional groups simultaneously present on carbonaceous particles were observed to be important for explaining their reactivity toward DTT. In particular,

strongly reduced surface functional groups (probed with NO_2) and carbonyls (probed with NH_2OH) were significant explanatory variables for the DTT consumption. By using oxidizing gas probes with different strength, different reducing surface functional groups can be titrated. NO_2 is a weak oxidizer compared to O_3, therefore NO_2 heterogeneously interacts with but the strongest reducing surface functional groups. In contrast, O_3 interacts with all reducing groups, strong and weak (see Table S1 in Supporting Information for quantitative results). The uptake of NO_2 on 1, 2, 10-trihydroxyanthracene (THA) adsorbed on both silica gel as well as on a non-polar silica gel coated with C_{18} aliphatic hydrocarbon has been studied.[34] In both cases significant uptake of NO_2 on the adsorbed hydroquinone has been observed. In addition, a concomitant lower-limit of 35% yield of HONO has been measured for THA hydroquinone adsorbed on silica gel, thus indicating a redox reaction between NO_2 and adsorbed THA. These data suggest that the oxidized product of the NO_2/adsorbed THA interaction may be the corresponding quinone.

The observed correlation between the mass-based DTT reactivity of a panel of 6 carbonaceous particles and the strongly reducing surface functional groups (Figure S3 in Supporting Information) is an unambiguous sign that reducing surface functional groups are important in the present oxidation reactions by dissolved O_2. Such a reducing property of carbonaceous NPs has already been reported[35-37] as well as its importance for sustaining the redox cycling of 1,4-naphtoquinone[38] or inducing a toxic response *in vitro* for lung epithelial cells co-exposed to CB and iron oxide NP. [39, 40] The association presented in Figure S3 (Supporting Information) leads us also to the conclusion that the rate limiting step in the oxidation of DTT is related to the oxidation of reducing sites on the NP surface by dissolved O_2. Oxygen will concomitantly be

reduced in what seems to be a catalytic overall reaction in view of the comparison of the limiting number of surface reaction sites and the number of O_2 molecules consumed.

Table 2 presents the turnover of the catalyst (particles) as defined above by comparing the total number of O_2 molecules consumed with either the sum of weakly and strongly reducing sites on the NP surface (using O_3 as a strongly oxidizing probe gas) or the strongly reducing sites (using the weakly oxidizing probe gas NO_2). For all three particle types considered, the number of strongly reducing sites on the particle surface is less by a factor of 30 - 600 compared to the number of consumed O_2. The sum of reducing sites is significantly lower and comprised between 3 and 230, as expected, owing to the larger abundance of the sum of all reducing surface sites compared to the number of strongly reducing sites. The turnover number is largest for SRM 2975 which may have to do with its large relative ratio of the number of strongly reducing to the sum of all reducing sites of 0.39. For both FW2 and Printex 90 the corresponding ratios are 0.096 and 0.065, respectively (see Supporting Information, Table S1).

Table 2: Averaged yield of consumed O_2 relative to available sum of reducing sites (O_3 probe gas) and strongly reducing (NO_2 probe gas) sites on the NP surface with the standard deviation of the n independent measurements.

		Ratio	Ratio
Particle type	n	O_2 consumed/sum of reducing sites	O_2 consumed/strongly reducing sites
FW2	11	3±1	35±16
Printex 90	4	5±2	68±29
SRM 2975	4	234±98	607±253

We therefore have significantly more O_2 disappearing than available reactive reducing surface sites in both cases, which allows only one conclusion, namely that the surface functional groups

are not consumed but instead regenerated in a chain reaction. Such a redox cycling process is possible due to the reversible change of oxidation state of the catalyst. We therefore reject a 1:1 stoichiometric reaction between the expected reactive reducing NP surface sites and dissolved O_2 that would leave the NP surface totally oxidized.

In order to take into account the fact that PM assumes a catalytic role in the DTT – O_2 system, the following additional reactions (6) and (7) have to be introduced:

$$PM_{red} + O_2 \longrightarrow PM_{ox} + H_2O_2 \qquad (6)$$

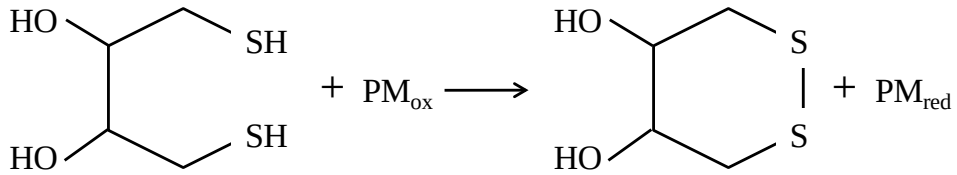

(7)

We attribute the initial oxidation of the reduced surface functional groups to the strongly reducing rather than to the sum of all reducing surface functional groups because the correlation of the DTT rate of disappearance with the number of surface functional groups reacting with NO_2 (N_{NO2}, displayed as abscissa in Figure S3 in the Supporting Information) is significantly better than with O_3 (N_{O3}).[24] Because the number of strongly reducing surface functional groups N_{NO2} is a subgroup of the sum of all reducing functional groups N_{O3}, the correlation of the rate of DTT disappearance with N_{O3} is preserved to some extent, albeit inferior to the correlation of the rate of DTT disappearance with the strongly reducing functional groups.

Rate Law for O_2 disappearance in the presence of carbonaceous NP substrates

The rate law and molecularity, that is the exponent of the concentration terms of the reaction partners in the rate law, is important information helping to unravel the reaction mechanism in terms of elementary reactions. The rate law for the disappearance of O_2 has the following general form for the present DTT – NP – O_2 system:

$$-d[O_2]/dt = k[O_2]^a\,[DTT]^b\,[NP]^c \qquad (8)$$

where $-d[O_2]/dt$ is taken at t = 0 at the start of the reaction, either right after addition of DTT or NP and is called the initial rate of reaction given by the tangent to the concentration vs. time curve (see Figure 1). The order of reaction or molecularity of the individual components are established by plotting log (d[X]/dt) vs. log $[O_2]$ or log [NP] at t = 0 when the concentrations of all reaction partners are known. The slope of the resulting straight line is the exponent *a* and *c*, respectively. Figure S4 in the Supporting Information displays experimental data for FW2 and Printex 90. For FW2 the slope $a = 1.96\pm0.24$ is measured and corresponds to a quadratic dependence on $[O_2]$ despite the modest range over which the O_2 concentration could be varied (approximately a factor of three, Figure 1). For Printex 90 the slope is 1.84±0.58, consistent with a value of two. Table S2 in the Supporting Information displays an analysis of the initial reaction rate upon DTT addition in the presence of FW2 and shows additional proof for the quadratic $[O_2]$ dependence of the initial rate. The exponent *c* is unity over the parameter space examined owing to the fact that we consistently observe a linear correlation of the initial rate with increasing NP mass as displayed in Figure 2. Regarding the molecularity of DTT we obtain b = 1.0 from data such as displayed in Figure S2 which reveals a linear dependence of the initial reaction rate as a function of DTT concentration which was varied by a factor of three. We therefore obtain the following overall rate law for the rate of O_2 consumption at a given initial DTT concentration:

$$-d[O_2]/dt = k\,[O_2]^2\,[DTT]\,[NP] \quad (9)$$

Figure 4 displays the absolute rate coefficients of the catalytic chain oxidation of DTT by dissolved oxygen in an aqueous suspension of carbonaceous nanoparticles at ambient temperature and pH = 7.0. Noteworthy is the significant difference in the rate coefficients for the three investigated NP's whereas the reaction stoichiometry seems to be similar for the NP's within experimental uncertainty as displayed in Figure 3.

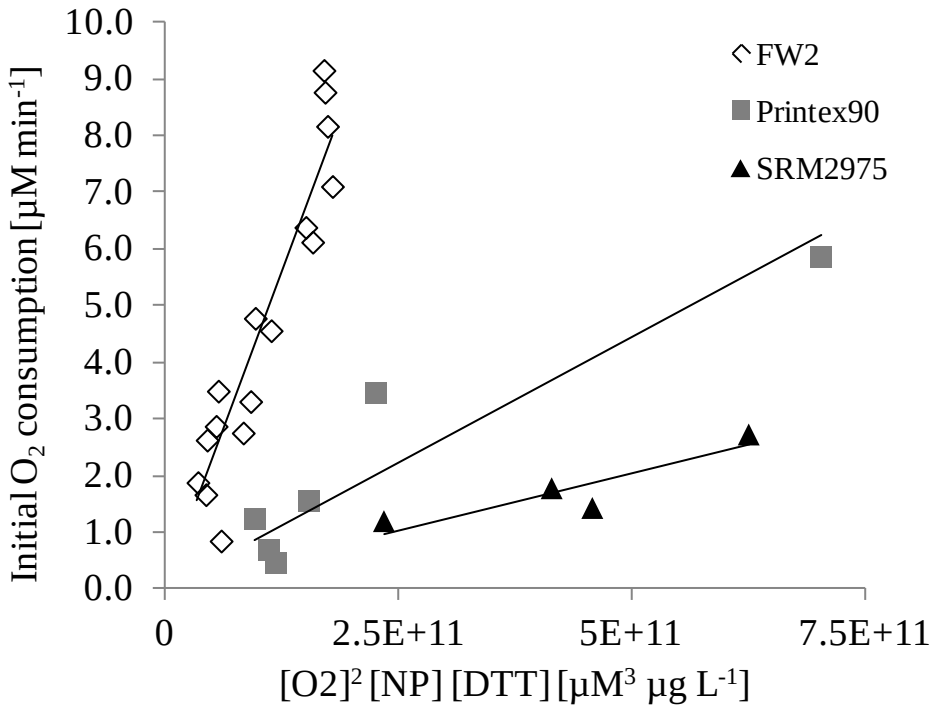

Figure 4: Experimentally determined initial rate of O_2 consumption divided by the products of the concentration terms displayed on the abscissa from the rate law displayed in equation (9). The slope corresponding to the absolute rate coefficients for the investigated NP's is 4.46 10^{-11} for FW2; 8.89 10^{-12} for Prinex 90 and 4.07 10^{-12} for SRM 2975.

Mechanistic considerations

Based on the observation that strongly reducing species are associated with the DTT consumption rate[24] (Figure S3in the Supporting Information), we propose that the reduction of molecular O_2 by strongly reducing surface functional groups on the particles is related to the rate limiting step in the system DTT – NP – O_2. Reactions (1), (2), (3), (6) and (7) each represent two-electron transfer steps and therefore do not correspond to elementary reactions. Electron transfer generally occurs as a rapid sequence of single electron steps even in cases where two-electron transfer reactions are experimentally observed owing to the fact that single electron transfer intermediates such as semiquinone radical anions have some thermodynamic stability.[41, 42] In addition, rate constants for reactions (1a) and 1(b) taking place in aqueous solutions have also been published together with accounts on general reactivity of semiquinone free radicals.[42,43] However, the quadratic dependence of the O_2 decay in the rate law in the presence of suspended particles cannot be explained by sequential steps of single-electron transfer processes. In the present case we have to invoke a heterogeneous reaction scheme taking place on the particulate surface following a Langmuir-Hinshelwood (LH) mechanism where two adsorbed $HO_2^{\bullet}$ free radicals collide on the surface in order to disproportionate according to equation (10). Based on the foregoing we are able to suggest the following molecular mechanism that is formulated without taking into account any loss of H_2O_2 by oxidation of the carbonaceous NP substrate (d = 1.0, see reactions (4) and (5)) discussed above according to equation (5). This elementary mechanisms is commonly known under the name of hydroquinone autoxidation.[42] In the following scheme equation (3) is not broken down into its elementary reactions:

$O_2 + PM_{red} \leftrightarrows PM^{\bullet}_{ox} + HO^{\bullet}_2(ads)$ (1 e^-) Heterogeneous Semiquinone formation (1a)

$O_2 + PM^{\bullet}_{ox} \leftrightarrows PM_{ox} + HO^{\bullet}_2(ads)$ (1 e^-) Heterogeneous Quinone formation (1b)

$2\,HO^{\bullet}_2(ads) \rightarrow H_2O_2 + O_2$ (1 e^-) Surface Disproportionation (Dismutation) (10)

$H_2O_2 + DTT \rightarrow DTT_{ox} + 2H_2O$ (2 e^-) Homogeneous Reduction of H_2O_2 by DTT (3)

$DTT + PM_{ox} \rightarrow DTT^{\bullet}_{ox} + PM^{\bullet}_{ox}$ (1 e^-) Heterogeneous Reduction of PM_{ox} (2a)

$DTT^{\bullet}_{ox} + PM^{\bullet}_{ox} \rightarrow DTT_{ox} + PM_{red}$ (1 e^-) Heterogeneous Regeneration of PM_{red} (2b)

$O_2 + 2\,DTT \rightarrow 2\,DTT_{ox} + 2H_2O$ Stoichiometry is invariant to mechanism change (A)

The quadratic dependence of the initial O_2 decay can only be explained by the bimolecular disproportionation reaction (10) occurring on the particle surface using the concept of a LH mechanism.[44] The rate-controlling step r being the slowest in the mechanism (reaction (10)) may be formulated as follows in the initial phases of reaction:

$$r = k_{eff}\,[HO_2^{\bullet}]_{ads}^{\,2} = k_{eff}^{\,'}\,K_{LH}^{\,2}[O_2]^2 \qquad (11)$$

where k_{eff} is the effective rate coefficient for reaction (10) at a given ratio of PM_{red} to PM_{ox} concentration that is thought to be invariant in time given the low coverage limit of O_2 on the NP surface. K_{LH} is the LH equilibrium constant, namely $K_{LH} = k_{ads}/k_{des}$ for the reversible adsorption/desorption of both O_2 to PM_{red} and O_2 to $PM_{ox}^{\bullet}$, the one-electron oxidized semiquinone free radical displayed in reactions (1a) and (1b). In the interest of simplicity we are treating both processes, namely equilibrium (1a) and (1b), alike using the identical LH-equilibrium constant K_{LH}. We are making the assumption that we express the LH kinetics in the sparsely covered surface limit because we reckon that only a small fraction of the adsorption sites of the NP is covered by molecular oxygen such that both PM_{red} and PM_{ox} do not vary with time. In the above mechanism all elementary processes are heterogeneous in nature because they

all involve the original or chemically modified surface sites except reaction (10) that could release H_2O_2 into the aqueous solution. However, it is at present not clear whether or not reaction (10) has heterogeneous components or not corresponding to adsorbed hydrogen peroxide because we have not probed for H_2O_2. In case the sparsely covered surface limit does not hold owing to significant surface coverage of $[HO_2^{\bullet}]_{ads}$ we must use the following limit that will somewhat reduce the quadratic dependence of r on $[O_2]$:

$$r = k_{eff}^{'} (K_{LH}^2[O_2]^2/(1 + 2K_{LH}^2[O_2]))^2 \quad (12)$$

Here again we are making the simplifying assumption that both LH-equilibrium constants are identical. If this assumption is relaxed, the term K_{LH}^2 must be replaced by the product of both LH constants for each individual equilibrium (equations (1a), (1b)). In addition, under these circumstances the ratio of PM_{red} to PM_{ox} cannot be expected to be constant such that a complex rate law will result.

In agreement with both the rate law, equation (9) and the correlation displayed in Figure S3 (Supporting Information), the slowest, that is the rate-limiting step, is the oxidation of the strongly reduced surface functional group which we tentatively identify with a polycyclic hydroquinone. The stability of a sequence of polycyclic aromatic hydroquinones significantly decreases with increasing annellation when compared to the corresponding quinones.[45] Owing to the waning stability of complex polycyclic hydroquinones the population on any given surface will be small, therefore the rate of the corresponding reaction (1a) will also be small to the extent that it is related to the rate-limiting step, equation (10), in the whole catalytic chain mechanism displayed above. In addition, $HO_2^{\bullet}$ free radical disproportionation (dismutation) reactions are notoriously slow in homogeneous solutions and therefore also rate-limiting.[21]

Tentative Identity of Redox Catalyst

In addition to transition metals,[11, 23, 46, 47] adsorbed quinones or quinone-like structures are often advocated to be the particulate components giving rise to catalytic redox activity and are thus considered important for understanding the ROS generation potential of PM.[5, 17] Simple aromatic quinones have been shown to redox cycle in the presence of O_2 and reducing species like DTT[5, 12, 16, 48] or ascorbic acid.[32, 38, 49] They cycle between quinone (conjugated di-carbonyl), semi-quinone (resonance-stabilized free radical) and hydroquinone (aromatic dihydroxy) structures. Quinones are minor components of PM[50-52] but due to their redox cycling ability,[53] they can be quite efficient in the formation of oxygen-containing conjugated free radicals. In the case of standard diesel soot SRM 2975 extracted with toluene, low concentrations of adsorbed 1,2-naphtoquinone, 9,10-phenanthraquinone and 9,10-anthraquinone were measured (Supporting Information, Table S3). Nevertheless, the contribution of these extractable quinoid species to the total DTT redox activity has been reported to be modest in the case of SRM 2975.[9, 54] However, the focus of the present work is the *in situ* investigation of the surface reactivity of carbonaceous NP's as opposed to extraction of reactive and extractable adsorbates. The comparison of the redox reactivity of NP's extracts with the *in situ* surface probing presented in this work is difficult because of the possibility of potential modifications of the redox reactivity upon solvent extraction.[55]

The insoluble black carbon core, corresponding to aromatic amorphous or graphene structures, might also present additional DTT reactivity.[8, 9, 56] Depending on the defects present on such graphene structures, different amount of oxygen can be incorporated,[57] possibly as carbonyl surface functional groups which may be able to catalytically and reversibly transfer electrons from DTT to O_2 in redox reactions. Such carbonyl functions on aromatic graphene structures

(vinylog) are exemplified in Figure 5. These structures preserve the properties of quinones and hydroquinones for large polycyclic aromatic hydrocarbons (PAH) approaching the limit of substituted graphenes.[58] A vinylogous quinone is a structure having two carbonyl groups at the periphery (circumference) in conjugation with each other through the molecular framework, thereby preserving the aromatic electronic resonance across the structure. Double bonds may thus be shifted without leading to unpaired, high-energy, electronic configurations. Up to 18% of the oxygen found on carbon blacks has been reported to be present in the form of a 1,4-quinone.[58] Figure 5 also shows that only carefully selected topologies satisfy the criterion of vinylogous resonances for two carbonyl groups usually attached to different annellated benzene rings. In contrast, there is no restriction on topology when dealing with the hydroquinone structure. The presence of a quinone-like structure in the three investigated particles is suggested by the fact that carbonyl surface functions were detected in significant amounts on the surface of the investigated particles by titrating them with NH_2OH in a Knudsen cell (Table S1, Supporting Information). Such surface functions have been reported to be also involved in DTT reactivity.[24] Additionally, the FTIR bands centered around 1600 cm^{-1} also support such structures (Figure S5, Supporting Information) and could be consistent with the presence of quinones in/on the NP's.

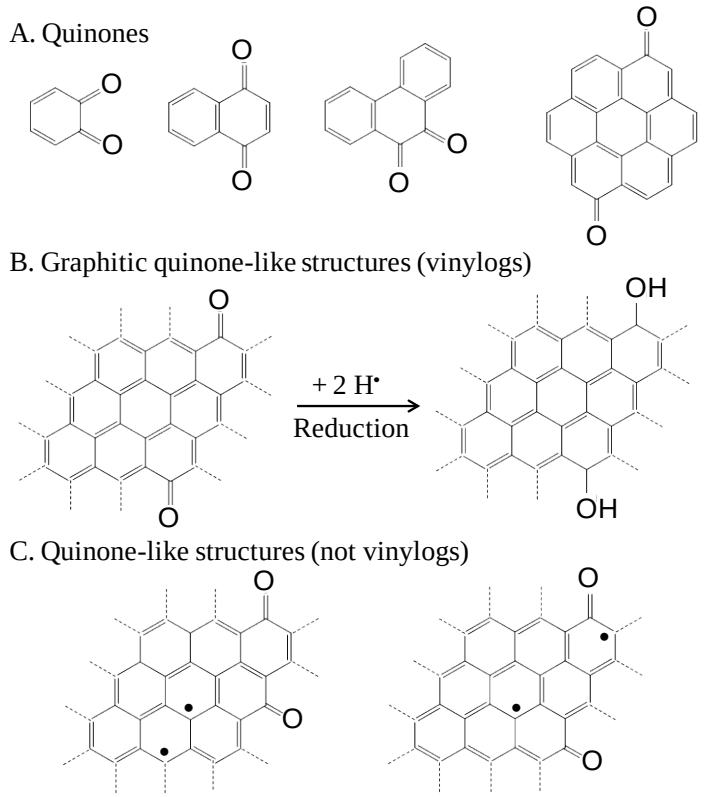

Figure 5: Example of **A**: Some low molecular weight quinone structures extractable from diesel particulates; **B**: vinylogous quinone-like structures. The dotted lines indicate adjacent aromatic structure; **C**: Topological structures which are not vinylogous correspond to high-energy (excited) forms. The topological position of the carbonyl groups in the quinone controls the positions of the conjugated double bonds in the aromatic hydrocarbon whereas there are no topological constraints for the hydroxyl groups of the corresponding hydroquinones at the periphery of the conjugated aromatic system.

In conclusion, we have shown for three carbonaceous NP's generated in a combustion process (soot) that they act as catalysts for oxidation of a typical reducing agent (DTT) in aqueous solution by atmospheric O_2. The rate-limiting step in the catalytic redox cycle seems to be the oxidation of reduced surface functional groups such as hydroquinones of large conjugated

aromatic hydrocarbons by dissolved O_2 (Figure S3, Supplemental Material). This result suggests that one should not exclusively consider the oxidative capacity of the NP interface as far as reaction kinetic is concerned. Rather, the presence of surface functional groups in a reduced state is necessary in order to enable the redox cycle (hydroquinone autoxidation) as we have found in this study. This has often been overlooked in the literature. The important particulate surface functional groups responsible for the catalytic activity of these NP's and the ROS generation are those able to be oxidized by O_2 and subsequently reduced by DTT in order to enable the catalytic chain reaction. Such a mechanism of sustained redox cycling may be relevant in relation to the health perspectives of carbonaceous NP's. As the particles deposited in the lung will encounter a reducing milieu,[3] reactions similar to the one described in this study may perhaps take place in the lung. Akin to NO_2, that acts as a catalyst in tropospheric ozone formation in the presence of oxidizable hydrocarbons, excess oxygen and sunlight, soot NP's may play an analogous role in the oxidation of antioxidants present in the aqueous phase covering the lung alveoli. In both situations the environmentally sound strategy must be the elimination of the catalysts in order to prevent or significantly slow down atmospheric oxidation processes. Additional research is nevertheless needed to probe the generality of such processes by extending the investigations to other types of NP's and to enlarge the probed parameter space.

ASSOCIATED CONTENT

SUPPORTING INFORMATION

Description of the oxygen consumption system, complementary kinetic data for DTT and O_2 consumption , extractable quinone content of SRM 2975 reference material and FTIR spectra are given. This information is available free of charge via the Internet at http://pubs.acs.org/.

AUTHOR INFORMATION

The manuscript was written from contributions of both authors. Both authors have given approval to the final version of the manuscript. The authors declare no competing financial interest.

ACKNOWLEDGMENT

MJR sincerely thanks Professors Urs Baltensperger and Alexander Wokaun, both of PSI, for institutional support regarding the experiments performed at PSI. The French Agence Nationale de Sécurité Sanitaire de l'Alimentation, de l'Environnement et du Travail (ANSES) is acknowledged for its financial support through grant EST 2006/1/7. The three anonymous reviewers are also acknowledged for their help in improving the manuscript.

REFERENCES

(1) Ayres, J. G.; Borm, P.; Cassee, F. R.; Castranova, V.; Donaldson, K.; Ghio, A.; Harrison, R. M.; Hider, R.; Kelly, F.; Kooter, I. M.; Marano, F.; Maynard, R. L.; Mudway, I.; Nel, A.; Sioutas, C.; Smith, S.; Baeza-Squiban, A.; Cho, A.; Duggan, S.; Froines, J. Evaluating the toxicity of airborne particulate matter and nanoparticles by measuring oxidative stress potential - A workshop report and consensus statement. *Inhal Toxicol* **2008**, 20 (1), 75-99.

(2) Nel, A.; Xia, T.; Madler, L.; Li, N. Toxic potential of materials at the nanolevel. *Science* **2006**, 311 (5761), 622-627.

(3) Cross, C. E.; Vandervliet, A.; Oneill, C. A.; Louie, S.; Halliwell, B. Oxidants, Antioxidants, and Respiratory-Tract Lining Fluids. *Environ. Health Perspect.* **1994**, 102, 185-191.

(4) Kelley, M. A.; Hebert, V. Y.; Thibeaux, T. M.; Orchard, M. A.; Hasan, F.; Cormier, S. A.; Thevenot, P. T.; Lomnicki, S. M.; Varner, K. J.; Dellinger, B.; Latimer, B. M.; Dugas, T. R. Model Combustion-Generated Particulate Matter Containing Persistent Free Radicals Redox Cycle to Produce Reactive Oxygen Species. *Chem. Res. Toxicol*. **2013**, 26 (12), 1862-1871.

(5) Antinolo, M.; Willis, M. D.; Zhou, S.; Abbatt, J. P. D. Connecting the oxidation of soot to its redox cycling abilities. *Nature Communications* **2015**, 6; DOI 10.1038/ncomms7812.

(6) Squadrito, G. L.; Cueto, R.; Dellinger, B.; Pryor, W. A. Quinoid redox cycling as a mechanism for sustained free radical generation by inhaled airborne particulate matter. *Free Radic. Biol. Med.* **2001**, 31 (9), 1132-1138.

(7) Cho, A. K.; Sioutas, C.; Miguel, A. H.; Kumagai, Y.; Schmitz, D. A.; Singh, M.; Eiguren-Fernandez, A.; Froines, J. R. Redox activity of airborne particulate matter at different sites in the Los Angeles Basin. *Environ. Res.* **2005**, 99 (1), 40-47.

(8) Pan, C. J. G.; Schmitz, D. A.; Cho, A. K.; Froines, J.; Fukuto, J. M. Inherent redox properties of diesel exhaust particles: Catalysis of the generation of reactive oxygen species by biological reductants. *Toxicol. Sci.* **2004**, 81 (1), 225-232.

(9) McWhinney, R. D.; Badali, K.; Liggio, J.; Li, S.-M.; Abbatt, J. P. D. Filterable Redox Cycling Activity: A Comparison between Diesel Exhaust Particles and Secondary Organic Aerosol Constituents. *Environ. Sci. Technol.* **2013**, 47 (7), 3362-3369.

(10) Donaldson, K.; Stone, V.; Seaton, A.; MacNee, W. Ambient particle inhalation and the cardiovascular system: Potential mechanisms. *Environ. Health Perspect.* **2001**, 109, 523-527.

(11) Charrier, J. G.; Anastasio, C. On dithiothreitol (DTT) as a measure of oxidative potential for ambient particles: evidence for the importance of soluble transition metals. *Atmos. Chem. Phys.* **2012**, 12 (19), 9321-9333.

(12) Kumagai, Y.; Koide, S.; Taguchi, K.; Endo, A.; Nakai, Y.; Yoshikawa, T.; Shimojo, N. Oxidation of proximal protein sulfhydryls by phenanthraquinone, a component of diesel exhaust particles. *Chem. Res. Toxicol.* **2002**, 15 (4), 483-489.

(13) Hirano, S.; Furuyama, A.; Koike, E.; Kobayashi, T. Oxidative-stress potency of organic extracts of diesel exhaust and urban fine particles in rat heart microvessel endothelial cells. *Toxicology* **2003**, 187 (2-3), 161-170.

(14) Penning, T. M.; Burczynski, M. E.; Hung, C. F.; McCoull, K. D.; Palackal, N. T.; Tsuruda, L. S. Dihydrodiol dehydrogenases and polycyclic aromatic hydrocarbon activation: Generation of reactive and redox active o-quinones. *Chem. Res. Toxicol.* **1999**, 12 (1), 1-18.

(15) Delgado-Saborit, J. M.; Alam, M. S.; Pollitt, K. J. G.; Stark, C.; Harrison, R. M. Analysis of atmospheric concentrations of quinones and polycyclic aromatic hydrocarbons in vapour and particulate phases. *Atmos. Environ.* **2013**, 77, 974-982.

(16) Dellinger, B.; Loninicki, S.; Khachatryan, L.; Maskos, Z.; Hall, R. W.; Adounkpe, J.; McFerrin, C.; Truong, H. Formation and stabilization of persistent free radicals. *Proc. Combust. Inst.* **2007**, 31, 521-528.

(17) Gehling, W.; Khachatryan, L.; Dellinger, B. Hydroxyl Radical Generation from Environmentally Persistent Free Radicals (EPFRs) in PM2.5. *Environ. Sci.Technol.* **2014**, 48 (8), 4266-4272.

(18) Valavanidis, A.; Iopoulos, N.; Gotsis, G.; Fiotakis, K. Persistent free radicals, heavy metals and PAHs generated in particulate soot emissions and residue ash from controlled combustion of common types of plastic. *J. Hazard Mater.* **2008**, 156 (1-3), 277-284.

(19) Khachatryan, L.; McFerrin, C. A.; Hall, R. W.; Dellinger, B. Environmentally Persistent Free Radicals (EPFRs). 3. Free versus Bound Hydroxyl Radicals in EPFR Aqueous Solutions. *Environ. Sci.Technol.* **2014**, 48 (16), 9220-9226.

(20) Lal, M.; Rao, R.; Fang, X. W.; Schuchmann, H. P.; von Sonntag, C. Radical-induced oxidation of dithiothreitol in acidic oxygenated aqueous solution: A chain reaction. *J. Am. Chem. Soc.* **1997**, 119 (24), 5735-5739.

(21) Zhang, N.; Schuchmann, H. P.; von Sonntag, C. The reaction of superoxide radical-anion with dithiothreitol. A chain process. *J. Phys. Chem.* **1991**, 95 (12), 4718-4722.

(22) Kachur, A. V.; Held, K. D.; Koch, C. J.; Biaglow, J. E. Mechanism of production of hydroxyl radicals in the copper-catalyzed oxidation of dithiothreitol. *Radiat. Res.* **1997**, 147 (4), 409-415.

(23) Netto, L. E. S.; Stadtman, E. R. The iron-catalyzed oxidation of dithiothreitol is a biphasic process: Hydrogen peroxide is involved in the initiation of a free radical chain of reactions. *Arch. Biochem. Biophys.* **1996**, 333 (1), 233-242.

(24) Sauvain, J.-J.; Rossi, M. J.; Riediker, M. Comparison of Three Acellular Tests for Assessing the Oxidation Potential of Nanomaterials. *Aerosol Sci.Technol.* **2013**, 47 (2), 218-227.

(25) *Certificate of analysis. Standard Reference Material 2975. Diesel Particulate Matter (Industrial Forklift)*. NIST: Gaithersburg, MD 20899, 2013.

(26) Sauvain, J. J.; Deslarzes, S.; Riediker, M. Nanoparticle reactivity toward dithiothreitol. *Nanotoxicology* **2008**, 2 (3), 121-129.

(27) Donaldson, K.; Beswick, P. H.; Gilmour, P. S. Free radical activity associated with the surface of particles: A unifying factor in determining biological activity? *Toxicol. Lett.* **1996**, 88 (1-3), 293-298.

(28) MacNee, W.; Donaldson, K. Mechanism of lung injury caused by PM10 and ultrafine particles with special referance to COPD. *Eur. Respir. J.* **2003**, 21, 47S-51S.

(29) Setyan, A.; Sauvain J.J.; Rossi M.J. The use of heterogeneous chemistry for the characterization of functional groups at the gas/particle interface of soot and TiO_2 nanoparticles *Phys. Chem. Chem. Phys*. **2009**, 11 (29), 6205-6217.

(30) Sander, R. Compilation of Henry's law constants (version 4.0) for water as solvent. *Atmos. Chem. Phys.* **2015**, 15 (8), 4399-4981.

(31) Halliwell, B.; Clement, M. V.; Long, L. H. Hydrogen peroxide in the human body. FEBS Lett. **2000**, 486 (1), 10-13.

(32) Roginsky, V. A.; Barsukova, T. K.; Stegmann, H. B. Kinetics of redox interaction between substituted quinones and ascorbate under aerobic conditions. *Chem. Biol. Interact.* **1999**, 121 (2), 177-197.

(33) Radi, R.; Beckman, J. S.; Bush, K. M.; Freeman, B. A. Peroxynitrite oxidation of sulfhydryls-The cytotoxic potential of superoxide and nicric-oxide. *J. Biol. Chem.* **1991**, 266 (7), 4244-4250.

(34) Stadler, D. A laboratory study of heterogeneous reactions relevant to the atmospheric boundary layer: soot as a reactive substrate. Ph.D Dissertation, EPFL, Lausanne, Switzerland, 2000.

(35) Strelko, V. V.; Kartel, N. T.; Dukhno, I. N.; Kuts, V. S.; Clarkson, R. B.; Odintsov, B. M. Mechanism of reductive oxygen adsorption on active carbons with various surface chemistry. *Surf. Sci.* **2004**, 548 (1-3), 281-290.

(36) Fu, R. W.; Zeng, H. M.; Lu, Y. The reduction property of activated carbon-fibers. *Carbon* **1993**, 31 (7), 1089-1094.

(37) Miljevic, B.; Heringa, M. F.; Keller, A.; Meyer, N. K.; Good, J.; Lauber, A.; Decarlo, P. F.; Fairfull-Smith, K. E.; Nussbaumer, T.; Burtscher, H.; Prevot, A. S. H.; Baltensperger, U.; Bottle, S. E.; Ristovski, Z. D. Oxidative Potential of Logwood and Pellet Burning Particles Assessed by a Novel Profluorescent Nitroxide Probe. *Environ. Sci.Technol.* **2010**, 44 (17), 6601-6607.

(38) Shang, Y.; Chen, C.; Li, Y.; Zhao, J.; Zhu, T. Hydroxyl Radical Generation Mechanism During the Redox Cycling Process of 1,4-Naphthoquinone. *Environ. Sci.Technol.* **2012**, 46 (5), 2935-2942.

(39) Guo, B.; Zebda, R.; Drake, S. J.; Sayes, C. M. Synergistic effect of co-exposure to carbon black and Fe2O3 nanoparticles on oxidative stress in cultured lung epithelial cells. *Part. Fibre Toxicol.* **2009**, 6; DOI 10.1186/1743-8977-6-4

(40) Berg, J. M.; Ho, S.; Hwang, W.; Zebda, R.; Cummins, K.; Soriaga, M. P.; Taylor, R.; Guo, B.; Sayes, C. M. Internalization of Carbon Black and Maghemite Iron Oxide Nanoparticle Mixtures Leads to Oxidant Production. *Chem. Res. Toxicol.* **2010**, 23 (12), 1874-1882.

(41) Kim, R. S.; Chung, T. D. The Electrochemical Reaction Mechanism and Applications of Quinones. *Bull. Korean Chem. Soc.* **2014**, 35 (11), 3143-3155.

(42) Song, Y.; Buettner, G. R. Thermodynamic and kinetic considerations for the reaction of semiquinone radicals to form superoxide and hydrogen peroxide. *Free Radic. Biol. Med.* **2010**, 49 (6), 919-962.

(43) McFerrin, C. A.; Hall, R. W.; Dellinger, B. Ab initio study of the formation and degradation reactions of semiquinone and phenoxyl radicals. *Theochem.* **2008**, 848 (1-3), 16-23.

(44) Laidler, K. *Chemical Kinetics*; Harper, Collins and Row: New York, 1987.

(45) Clar, E. *Aromatische Kohlenwasserstoffe, Polycyclische Systeme*; Springer Verlag Berlin, 1952.

(46) Held, K. D.; Biaglow, J. E. Role of copper in the oxygen radical-mediated toxicity of the thiol-containing radioprotector dithiothreitol in mammalian cells. *Radiat. Res.* **1993**, 134 (3), 375-382.

(47) Held, K. D.; Biaglow, J. E. Mechanisms for the Oxygen Radical-Mediated Toxicity of Various Thiol-Containing Compounds in Cultured-Mammalian-Cells. *Radiat. Res.* **1994**, 139 (1), 15-23.

(48) Wang, Y.; Arellanes, C.; Paulson, S. E. Hydrogen Peroxide Associated with Ambient Fine-Mode, Diesel, and Biodiesel Aerosol Particles in Southern California. *Aerosol Sci. Technol.* **2012**, 46 (4), 394-402.

(49) Li, Y.; Zhu, T.; Zhao, J.; Xu, B. Interactive Enhancements of Ascorbic Acid and Iron in Hydroxyl Radical Generation in Quinone Redox Cycling. *Environ. Sci.Technol.* **2012**, 46 (18), 10302-10309.

(50) Cho, A. K.; Di Stefano, E.; You, Y.; Rodriguez, C. E.; Schmitz, D. A.; Kumagai, Y.; Miguel, A. H.; Eiguren-Fernandez, A.; Kobayashi, T.; Avol, E.; Froines, J. R. Determination of four quinones in diesel exhaust particles, SRM 1649a, an atmospheric PM2.5. *Aerosol Sci. Technol.* **2004**, 38, 68-81.

(51) Chung, M. Y.; Lazaro, R. A.; Lim, D.; Jackson, J.; Lyon, J.; Rendulic, D.; Hasson, A. S. Aerosol-borne quinones and reactive oxygen species generation by particulate matter extracts. *Environ. Sci.Technol.* **2006**, 40 (16), 4880-4886.

(52) Jakober, C. A.; Riddle, S. G.; Robert, M. A.; Destaillats, H.; Charles, M. J.; Green, P. G.; Kleeman, M. J. Quinone emissions from gasoline and diesel motor vehicles. *Environ. Sci.Technol.* **2007**, 41 (13), 4548-4554.

(53) Valim, R. B.; Reis, R. M.; Castro, P. S.; Lima, A. S.; Rocha, R. S.; Bertotti, M.; Lanza, M. R. V. Electrogeneration of hydrogen peroxide in gas diffusion electrodes modified with tert-butyl-anthraquinone on carbon black support. *Carbon* **2013**, 61, 236-244.

(54) Akhtar, U. S.; McWhinney, R. D.; Rastogi, N.; Abbatt, J. P. D.; Evans, G. J.; Scott, J. A. Cytotoxic and proinflammatory effects of ambient and source-related particulate matter (PM) in relation to the production of reactive oxygen species (ROS) and cytokine adsorption by particles. *Inhal. Toxicol.* **2010**, 22, 37-47.

(55) Yang, A.; Jedynska, A.; Hellack, B.; Rooter, I.; Hoek, G.; Brunekreef, B.; Kuhlbusch, T. A. J.; Cassee, F. R.; Janssen, N. A. H. Measurement of the oxidative potential of PM2.5 and its constituents: The effect of extraction solvent and filter type. *Atmos. Environ.* **2014**, 83, 35-42.

(56) Shinyashiki, M.; Eiguren-Fernandez, A.; Schmitz, D. A.; Di Stefano, E.; Li, N.; Linak, W. P.; Cho, S. H.; Froines, J. R.; Cho, A. K. Electrophilic and redox properties of diesel exhaust particles. *Environ. Res.* **2009**, 109 (3), 239-244.

(57) Mueller, J. O.; Su, D. S.; Wild, U.; Schlögl, R. Bulk and surface structural investigations of diesel engine soot and carbon black. *Phys. Chem. Chem. Phys.* **2007**, 9 (30), 4018-4025.

(58) Hallum, J. V.; Drushel, H. V. The organic nature of carbon black surfaces. *J. Phys. Chem.* **1958**, 62 (1), 110-117.